Vietnam Journal of Science and Technology ***57*** *(3A) (2019) 41-47*
doi:10.15625/2525-2518/57/3A/14057

TEMPERATURE-DEPENDENT PHOTOLUMINESCENCE STUDY OF POROUS GaP

Pham Thi Thuy

Department of Natural Sciences Education, Sai Gon University
273 An Duong Vuong Road, Ward 3, Distrist 5, Ho Chi Minh City

*Email: *phamthithuy@sgu.edu.vn*

Received: 30 July 2019, Accepted for publication: 5 September 2019

Abstract. This paper reports on the temperature-dependent photoluminescence of porous GaP under the 355-nm excitation. Porous GaP was formed by electrochemical anodization of the (111)-oriented bulk material. Photoluminescence taken from the porous GaP at room temperature shows a narrow green emission band peaking at 550 nm (2.25 eV) and a broad red emission one peaking at 770 nm (1.65 eV). In the temperature range from 25 K to 275 K intensity from the green emission gradually decreases with increasing temperature. Additionally, the red-shift of the green luminescence band with increasing temperature exhibits the same that of the GaP band gap narrowing with temperature. This means a contribution of the phonons and the lattice dilatation with the increase of temperature.

Keywords: porous GaP, temperature-dependent photoluminescence.

Classification numbers: 2.1.3, 2.4.1.

1. INTRODUCTION

Porous semiconductors are attracting research interest because of their interesting physical properties. Porous silicon was discovered in 1957 by Uhlin due to the observation of visible room-temperature luminescence [1]. This material plays an important role in many technologies such as optical and photonic devices [2, 3], sensors [4-6], (bio) chemical reactors [7] and super capacitors [8]. Like silicon, III-V semiconductor such as gallium phosphide has been investigated in the form of porous structure [9-13]. GaP can be made porous by anodic etching in 25 % HF electrolyte of (111)-oriented bulk material. This material has an indirect band gap (2.24 eV) and its band structure is similar to that of silicon. These make porous GaP a very promising photonic material for the visible spectral range. In the photoluminescence (PL) spectra of this porous sample, it is observed not only emission peak originating from the excitonic transition but also the one resulting from radiative recombination via donor – acceptor pairs [9,10]. These emission bands have been typically observed in bulk GaP but photoluminescence intensity is much lower than porous GaP. To date, the enhancement of photoluminescence intensity of porous GaP is still a mystery, probably related to surface states [9,11]. Therefore, it is necessary to study systematically porous GaP by means of steady-state

and time-resolved photoluminescence (TRPL) in order to know their optical characteristics in detail.

In this paper, we highlight the results on the temperature-dependent time-resolved photoluminescence (TRPL) of porous GaP semiconductor. In the temperature range from 25 K to 275 K intensity from the exciton emission gradually decreases when the temperature increases. And peak position of this emission red-shifts gradually with an increase in the temperature, the same as the energy shift of the GaP bandgap. This means that even with a very small assemble of atoms to form microcrystals the temperature-dependence of energy levels takes place the same as in the bulk, meaning the contribution of the microfield induced by lattice vibrations.

3. EXPERIMENT

2.1. Chemicals

Hydrofluoric acid (HF, 48 %) was purchased from Merck; ethanol (C_2H_5OH, 98 %) was purchased from Beijing Pure Chem. China. These chemicals were directly used as purchased from companies without any further purification.

2.2. Fabrication of porous GaP

Gallium phosphide was made porous by electrochemical anodic etching of single-crystalline GaP in electrolyte. Experiment was performed at room temperature. An n-GaP substrate in the (111) orientation, doped with tellurium to a carrier density $n = 3 \times 10^{17}$ cm^{-3} was used. The semiconductor was placed in a holder that was designed to make an electrical connection to the back side using an aluminum plate. A potential was applied between the semiconductor electrode and a platinum counter electrode. A plot of the current through the GaP was measured at the function of the applied potential. The porous sample was formed by etching of GaP in an electrochemical cell at current density 2.73 mA/cm^2 for 15 min. The electrolyte used in this experiment was a 25 % solution of HF in methanol.

2.3. Measurements

Scanning electron microscopy (SEM) (S-4800 Hitachi) enabled us to determine directly the size and shape of pores of porous GaP.

In both steady-state PL and TRPL measurements, the 355-nm laser line, which is above the GaP transition energy was used as the excitation source. The photoluminescence signals were dispersed by using a 0.55-m grating monochromator (Horiba iHR550) and then detected by a thermoelectrically cooled Si-CCD camera (Synapse). The TRPL signals were dispersed by using a 0.6-m grating monochromator (Jobin-Yvon HRD1) and then detected using a fast photomultiplier (Hamamatsu model H733, with the rise time of 700 ps). Averaging the multi-pulses at each spectral point using 1.5 GHz digital oscilloscope (LeCroy 3962) strongly improved the signal-to-noise ratio.

For the structural characterization of as-prepared sample, Raman scattering (RS) spectroscopy (Labram 1-B (Jobin-Yvon) spectrometer with the 632.8-nm laser light excitation) investigations were performed.

3. RESULTS AND DISCUSSION

The morphology of the obtained porous GaP has been characterized by scanning electron microscopy. The SEM image taken from a porous GaP is illustrated in Figure 1, in which the pores are pyramid in shape having a mean size around 1.5 μm.

To confirm the structure of the obtained porous GaP samples, we did Raman scattering measurement to get their spectra. The RS spectra (not shown) demonstrate the two peaks at around 365 cm^{-1} and peak at 404.2 cm^{-1}. The vibrational mode at around 365 cm^{-1} corresponds to TO phonon, while LO phonon vibration locates at 404.2 cm^{-1}, consistent with previous reports [9, 14-16]. It is important to note that the intensity of the scattering involving LO phonon in porous GaP is higher than that of bulk material and the LO-phonon peak is shifted to lower frequency (0.5 cm^{-1}) and broadened with a low-frequency shoulder. The observed changes in RS spectrum caused by anodization possibly give an evidence for increased surface-to-volume ratio in porous GaP [16].

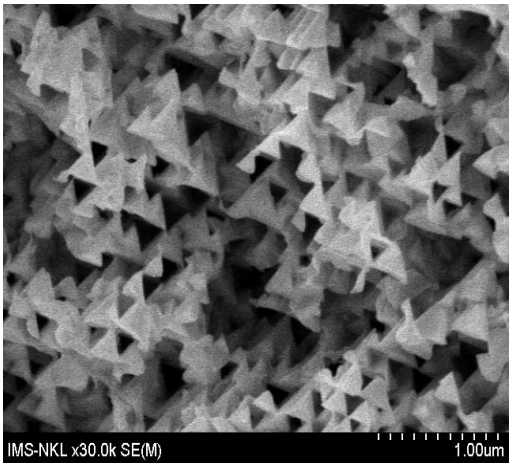

Figure 1. SEM image of porous GaP formed by etching GaP substrate at current density 2.73 mA/cm^2 for 15 min in 25 % HF solvent.

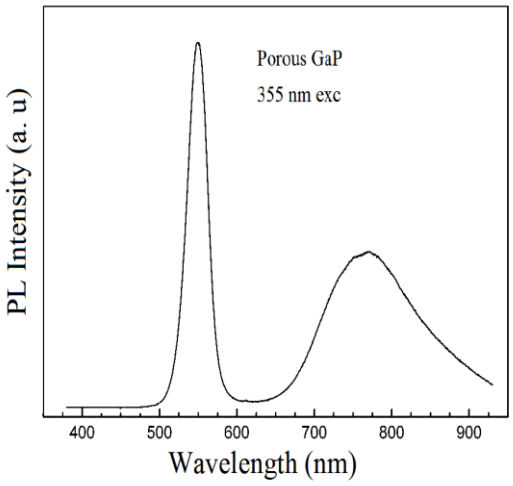

Figure 2. PL spectra of porous GaP under 355-nm excitation.

We now discuss the optical properties of porous GaP fabricated by electrochemical anodic etching. Figure 2 shows the steady-state PL spectra of porous GaP at room temperature under the 355-nm laser line excitation. We observed not only the narrow band peaking at 550 nm (2.25 eV) in the near-band-edge region of GaP, but also the broad one peaking in the red region at 770 nm (1.65 eV). The intense and narrow (35 nm at haft-maximum) green emission band peaking very close to the bandgap energy of GaP may be attributed to the radiative transition of excitons related to bulk GaP [16]. The broad (140 nm at haft-maximum) red emission band is interpreted as resulting from radiative recombination via donor – acceptor pairs (DAP) in the band gap [9, 10].

In the TRPL spectra, we observed only the green emission peaking at 550 nm (Figure 3). The absence of the red emission at 770 nm in the TRPL spectra is possibly due to its long luminescence decay time compared to that of the green one. From the steady-state PL spectrum (Figure 2), we see that the integral emission from the green and red bands are comparable. This helps to understand that the decay time of the exciton green emission is much shorter than that of the DAP red emission. Therefore, in the TRPL measurement, the instant PL intensity of the

green one is dominate at the short delay time after the laser pulse excitation, while that of the red one is too small. In other words, even though the steady-state integral PL of the green and red bands are comparable, the instant PL intensity of the red emission band at a short delayed time from the pulsed excitation can be hundreds of times less than that of the green emission band. However, by integrating in whole acquisition time like in the steady-state PL measurement, the PL integral intensity of the red band shows comparably with that of the green one. Figure 3 shows the TRPL spectra of green band at 2.25 eV of porous GaP under the 355-nm laser line excitation at various temperatures from 15 K to 275 K. We can see that the PL intensity of the green emission decreases when the temperature increases. In addition, its PL full width at haft maximum (FWHM) gradually narrows from 25 nm to 12 nm with a decrease in temperature from 275 K to 15 K. The red-shift emission with increasing temperature is essentially caused by the contribution of the microfield induced by lattice vibrations/phonons and by the lattice thermal expansion [17]. Because the phonon population is dependent on temperature, the microfields originating from them is also temperature-dependent. In fact, the bandgap energy of bulk semiconductors narrowed with increasing temperature is caused by the contributions mentioned above. It is interesting that even in the tiny objects like InP quantum dots [18] or GaP porous structure the microfield takes significantly place to cause the energy gap narrowing, giving rise to the red-shift of emissions with increasing temperature.

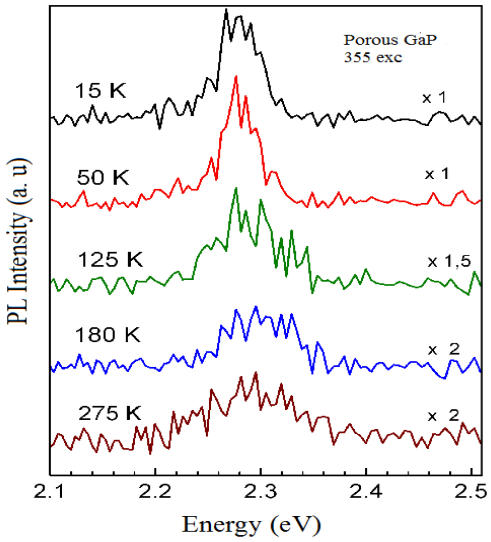

Figure 3. TRPL spectra of porous GaP as a function of temperature under 355-nm excitation.

For most bulk semiconductors, the evolution of the bandgap energy with temperature is well fit to Varshni's equation.

$$E(T) = E(0) - \frac{\alpha T^2}{\beta + T}$$

where $E(T)$ is the transition energy at temperature T, $E(0)$ is the transition energy at 0 K and α, β are the Varshni's coefficients. One can expect that the excitonic emission is evolved with temperature closely as that of the bandgap energy.

Figure 4 presents the peak position of the green PL component as a function of temperature. As mentioned above, the bandgap narrowing with temperature happens even in the tiny objects

because the microfield takes significantly place. For the case of porous GaP, the variations of the green emission peaks with temperature are fit to Varshni's equation. The gradual red-shift of the peak position with increasing sample temperature following the same the energy shift of the GaP bandgap with temperature. With an increase in the temperature from 15 K to 275 K, the red-shift of the peak position was determined about 50 meV. The best fit has yielded the values $E(0) =$ 2.278 eV, $\alpha = 3.6.10^{-4}$ eV/K, $\beta = 298$ K.

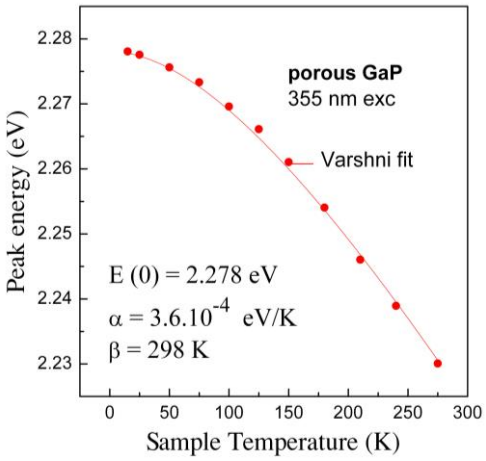

Figure 4. Peak position of PL spectra from porous GaP as a function of temperature under 355-nm excitation. Dots are experimental data. Line is the fit with Varshni's equation.

4. CONCLUSIONS

In conclusion, we have studied the temperature-dependence of photoluminescence from porous GaP by using the 355-nm light as the excitation source. The overall photoluminescence spectra show two spectral components, the green peak at 2.25 eV and the red peak at 1.65 eV, corresponding the excitonic transition and donor-acceptor pair recombination, respectively. Peak position of the green luminescence band shifts to lower energy with increasing temperature and the same the GaP band gap narrowing with temperature. In the temperature range from 25 K to 275 K intensity from the green emission gradually decreases when the temperature increases. These obtained results show that even with a very small assemble of atoms to form microcrystals the temperature-dependence of energy levels takes place the same as in the bulk, meaning the contribution of the microfield induced by lattice vibrations/phonons. On-going work is devoted to the analysis of the contribution of acoustic and optical phonons to the exciton emission of porous GaP.

Acknowledgements. The author would like to thank Prof. Nguyen Quang Liem and Prof. Bui Huy for their helpful discussions. I would like to express my gratitude to Dr. Tran Thi Kim Chi for guiding me in the photoluminescence measurement.

REFERENCES

1. Uhlir A. – Electrolytic shaping of germanium and silicon, Bell System Technical Journal **35** (1956) 333-347.

2. Loni A., Canham L. T., Berger M. G., Arens-Fischer R., Munder H., Arrand H. F., and Benson T. M. – Porous silicon multilayer optical waveguieds, Thin Solid Films **276** (1996) 143.
3. Remache L., Nychyporuk T., Guermit N., Fourmond E., Mahdjoub A., and Lemiti M. – Optical properties of porous Si/PECVD SiN_x:H reflector on single crystalline Si for solar cells, Materials Science-Poland **34** (1) (2016) 94-100.
4. Barillaro G., Diligenti A., Strambini L. M., Comini E., and Faglia G. – NO_2 adsorption effects on p + - n silicon junctions surrounded by a porous layer, Sens Actuator B **134** (2008) 922-927.
5. Barillaro G., Lazzerini G. M., and Strambini L. M. – Modeling of porous silicon junction field effect transition gas sensors: insight into NO2 interaction, Applied Physic Letter **96** (2010) 162105.
6. Barillaro G.,Bruschi P., Lazzerini G. M., and Strambini L. M. – Validation of the compatibility between a porous silicon-based gas sensor technology and standard microelectronic process, Sens J IEEE **10** (4) (2010) 893-899.
7. Drott J., Lindstrom K., Rosengren L., and Laurell T. - Porous silicon as the carrier matrix in micro structured enzyme reactor yielding enzyme activities, J. Micromech. Microeng. **7** (1997) 14-23.
8. Wang S., Ma F., Jiang H., Shao Y., Wu Y., and Hao X. - Band gap- tunable porous Borocarbonitride nanosheets for high energy- density supercapacitors, ACS Appl Mater Interfaces **10** (23) (2018) 19588-19597.
9. Belogorokhov A. I., Karavanskii V. A., Obraztsov A. N., and Timoshenko V. Y. - Intense photoluminescence in porous gallium phosphide, JETP Lett. **60** (1994) 274-279.
10. Tomioka K., and Adachi S. - Structural and photoluminescence properties of porous GaP formed by electrochemical etching,. J. App. Phys. **98** (2005) 073511.
11. Stevens-Kalceff M. A., Tiginyanu I. M., Langa S., Foll H. and Hartnagel H. L. - Correlation between morphology and cathodeluminescence in porous GaP, J. App. Phys. **89** (2001) 2560.
12. Masalov S. A., Atrashchenko A. V., Ulin V. P., Popov E. O., Kolosko A. G., and Filippov S. V. - A study of electrical properties of the porous GaP (111) surface, Technical Physics Letters **42** (11) (2016) 1118-1121.
13. Vambol S., Vambol V., Suchikova Y., Bogdanov I., and Kondratenko O. - Investigation of the porous GaP layers, chemical composition and the quality of the tests carried out, Journal of Achievements in Materials and Manufacturing Engineering **86** (2) (2018) 49-60.
14. Campbell L. H., and Fauchet P. M. - The effect of microcrystal size and shape on the one phonon Raman spcetra of crystalline semiconductors, Solid State Commum. **58** (10) (1986) 739-741.

15. Sarua A., Irmer G., Monecke J., Tiginyanu I. M., Schwab C., Grob J. J., and Hartnagel H. L. - Raman spectroscopy of porous and bulk GaP subjected to MeV-ion implantation and annealing, Journal of Applied Physic **88** (12) (2000) 7006-7012.
16. Anedda A., Serpi A., Karavanskii V. A., Tiginyanu I. M., and Ichizli V. M. - Time resolved blue and ultraviolet photoluminescence in porous GaP, Appl. Phys. Lett. **67** (22) (1995) 3316-3318.
17. Liem N. Q., Quang V. X., Thanh D. X., Lee J. I., and Kim D. - Temperature dependence of biexciton luminescence in cubic ZnS single crystals, Solid State Communications **117** (4) (2001) 255-259.
18. Thuy P. T., Chi T. T. K., and Liem N. Q. - Temperature-dependent photoluminescence study of InP/ZnS quantum dots, Adv. Nat. Sci.: Nanosci. Nanotechnol. **2** (2011) 025001.